*Evolutionary Ecology Research*, 2012, **14**: 125–146

# Evolution of host resistance towards pathogen exclusion: the role of predators

Andy Hoyle[1], Alex Best[2,3] and Roger G. Bowers[4]

[1]*School of Natural Sciences, University of Stirling, Stirling, UK,* [2]*School of Mathematics and Statistics, University of Sheffield, Sheffield, UK,* [3]*Biosciences, College of Life and Environmental Sciences, University of Exeter, Cornwall Campus, Penryn, UK and* [4]*Department of Mathematical Sciences, The University of Liverpool, Liverpool, UK*

## ABSTRACT

**Question:** Can increased host resistance drive a pathogen to extinction? Do more complex ecosystems lead to significantly different evolutionary behaviour and new potential extinctions?

**Mathematical method:** Merging host–parasite models with predator–prey models. Analytically studying evolution using adaptive dynamics and trade-off and invasion plots, and carrying out numerical simulations.

**Key assumptions:** Mass action (general mixing). All individuals of a given phenotype are identical. Only prey vulnerable to infection. Mutations are small and rare (however, the assumption on the size of mutation is relaxed later). In simulations, very small (negligible) populations are at risk of extinction.

**Conclusions:** The presence of the predator can significantly change evolutionary outcomes for host resistance to a pathogen and can create branching points where none occurred previously. The pathogen (and sometimes the predator) is protected from exclusion if we take mutations to be arbitrarily small; however, relaxing the assumption on mutation size can lead to its exclusion. Increased resistance can drive the predator and/or pathogen to extinction depending on inter-species dynamics, such as the predator's preference for infected prey. Predator co-evolution can move exclusion boundaries and prevent the predator's own extinction if its rate of mutation is high enough (with respect to that of the prey).

*Keywords*: adaptive dynamics, co-evolution, eco-epidemiology, extinction, parasite, singular strategy.

## 1. INTRODUCTION

Understanding the evolutionary dynamics of infectious diseases remains a key topic in evolutionary ecology and is central to our management of natural systems. Our theoretical understanding of the evolution of hosts and their parasites continues to grow (e.g. Levin and Pimental, 1981; Boots and Haraguchi, 1999; Best *et al.*, 2010b), yet researchers tend to assume that hosts and

Correspondence: A. Best, School of Mathematics and Statistics, University of Sheffield, Sheffield S3 7RH, UK. e-mail: a.best@shef.ac.uk

parasites interact in isolation. In reality, ecosystems consist of a complex mix of species, including hosts, parasites, predators, prey, competitors, and mutualists. Understanding how infectious disease dynamics are affected by the interference of this range of interacting species is clearly crucial for any predictions to be made in real systems.

Much of the theory on infectious disease systems has focused on the evolution of the parasite, investigating, for example, when disease may become endemic and when highly virulent parasites may be selected for (e.g. Anderson and May, 1981; Levin and Pimental, 1981; Pugliese, 2002; Svennungsen and Kisdi, 2009). In response to parasitism, hosts are clearly likely to experience strong selection to develop defence mechanisms, and there is a growing body of theory focusing on the evolution of the host (e.g. Frank, 1993; Boots and Bowers, 1999, 2004). Broadly, host defence may be divided into two sub-classes: resistance and tolerance. Resistance mechanisms, which act to directly harm the parasite, include avoidance of infection (Boots and Bowers, 1999; Boots and Haraguchi, 1999), clearance of disease (van Baalen, 1998; Boots and Bowers, 1999), and acquired immunity (Boots and Bowers, 2004), whereas tolerance mechanisms do not affect the parasite, but rather ameliorate parasite-induced damage (Boots and Bowers, 1999, 2004; Roy and Kirchner, 2000; Miller *et al.*, 2005). The differing feedbacks produced by these alternative defence mechanisms can result in very different behaviours (Boots, 2008; Boots *et al.*, 2009), such as allowing branching and co-existence of host strains when defence is through resistance but not when it is through tolerance (Roy and Kirchner, 2000; Miller *et al.*, 2005; but see Best *et al.*, 2010a).

While the evolution of both parasites and hosts – and, increasingly, their co-evolution (van Baalen, 1998; Dieckmann *et al.*, 2002; Restif and Koella, 2003; Best *et al.*, 2009) – is now well studied in relatively simple one-host/one-parasite systems, there has been little consideration of how interactions with other species may impact disease dynamics. In contrast, a number of predator–prey and competition models have shown that interacting species play an important role in their evolutionary dynamics (e.g. Kisdi, 1999; Bowers *et al.*, 2003; Hoyle *et al.*, 2008), although these do not include pathogens. In two recent exceptions, Morozov and Adamson (2011) and Morozov and Best (2012) studied an SI (susceptible–infected) model where predators fed on infected prey and found that the evolution of pathogen virulence changed due to the presence of a predator. Population studies have shown that these interactions, particularly predator–prey–infection (or eco-epidemiological) models, can have significant effects on the dynamics of species and on disease control strategies (e.g. Hudson and Greenman, 1998; Venturino, 2001, 2002; Haque *et al.*, 2009; Greenman and Hoyle, 2010; Haque and Greenhalgh, 2010). These include unbalancing competitive effects and driving one species to extinction, or in some cases allowing two species to co-exist where they would usually not be able to (Hudson and Greenman, 1998).

Much of the modern literature on the evolutionary ecology of hosts and parasites has been conducted within the framework of adaptive dynamics (Metz *et al.*, 1996a; Geritz *et al.*, 1998), which allows the study of trait substitution sequences resulting from the challenge of a resident strain by a closely similar mutant. One key feature of most of these studies is the evolutionary trade-off between beneficial mutations (for example, increased defence in the host) and fitness costs incurred elsewhere (for example, reduced reproductive ability). The shape of these evolutionary trade-offs has been found to be crucial to the outcomes of a range of ecological systems, and is now central to adaptive dynamics theory (de Mazancourt and Dieckmann, 2004; Rueffler *et al.*, 2004; Bowers *et al.*, 2005). Focusing on host evolution, where defence comes at accelerating costs (i.e. each additional unit of benefit is met by an increased cost), the system generally tends to an intermediate strategy that is a long-term attractor of evolution (or a continuously stable strategy), whereas where defence incurs decelerating costs, hosts may be driven to maximize or minimize defence due to an evolutionary repellor.

Trade-offs that are weakly accelerating or decelerating (or even linear) may display either behaviour, or may exhibit evolutionary branching, where the initial monomorphic population splits into two (or more) co-existing strains.

The main aim of this paper is to investigate the relevance of the relationship between trade-offs and evolutionary outcomes in the context of the evolution of host resistance to parasitism in the presence of an immune predator. In particular, we look into what trade-off shapes enhance the possibility of co-existence between species, potentially leading to branching and speciation, and what shapes lead to significant changes in the ecosystem with the eradication of pathogens and/or predators. We use the method of trade-off and invasion plots (TIPs) (Bowers *et al.*, 2005), which highlights the role of the trade-off in determining the evolutionary outcome, and thus intend to show the efficacy of this approach in such investigations. We also perform numerical simulations that allow the inclusion of some stochastic behaviour. We initially take a prey-only system, modelled by a standard SIS (susceptible–infected–susceptible) model and investigate the evolutionary behaviour of the system when host resistance (through decreased transmission) is costly to an aspect of the disease-free demography (decreased birth rate). In particular, we look at whether evolution of the host can exclude the pathogen. We then move on to include the immune predator in the system and look at how the evolutionary behaviour changes and if the predator can be excluded from the system. We initially do this by looking at evolution of the prey alone, before moving onto a co-evolutionary set-up where the prey and predator co-evolve.

## 2. THE MODEL

Our analysis is based on a predator–prey system where the prey is subject to a pathogen, modelled by an SIS set-up, but the predator is immune. We use the equations

$$\begin{aligned}\frac{dS}{dt} &= aH - qH^2 - bS - \beta SI + \gamma I - cSP\\ \frac{dI}{dt} &= \beta SI - (\alpha + b + \gamma)I - c\phi IP\\ \frac{dP}{dt} &= \theta cP(S + \phi I) - dP\end{aligned} \tag{1}$$

where $S$ and $I$ are the densities of susceptible and infected prey, with $H = S + I$, and $P$ is the density of predators. In addition, $a$ is the prey birth rate, $q$ is the rate of density-dependent competition (acting on births), $b$ is the natural prey death rate, $\beta$ is the transmission rate, $\alpha$ is the parasite-induced death rate or pathogenicity, $\gamma$ is the recovery rate, $c$ is the predation rate, $\phi$ represents the increase/decrease in predation rate suffered by infected individuals, $\theta$ relates to the conversion of predation into the births of new predators, and $d$ is the predator death rate.

## 3. PATHOGEN EXCLUSION: EVOLUTION OF RESISTANCE IN A PREY-ONLY ENVIRONMENT

We stress here that although we take $c = 0$ throughout this section, we leave it in the respective equations as we will later take $c > 0$ and refer back.

With respect to prey evolution and the algebraic analysis throughout this study, we assume that the host can evolve resistance to parasitism through reducing the transmission rate, $\beta$. Due to constraints, such as energetic ones (resource allocation), any benefit gained in one life-history trait must come at the cost of another and hence we assume a cost to resistance through reduced birth rate, with a trade-off $a = f(\beta)$ with $f > 0$. We take the trade-off to be of the form:

$$a = f(\beta) = f(1) - \frac{f'(1)^2}{f''(1)}\left(1 - e^{\frac{f''(1)}{f'(1)}(\beta - 1)}\right). \tag{2}$$

In each example, the value of $f'(1)$ is chosen to ensure that there is always a singular strategy at $\beta^* = 1$, with $a^* = 2$. (We see similar results for other choices.) All other parameters are taken to be constant. We take $a$ and $\beta$ to represent the traits of the resident strain, existing at a stable equilibrium with densities $S = S(a, \beta)$ and $I = I(a, \beta)$ (later co-existing with a predator at density $P = P(a, \beta)$), and $\hat{a}$ and $\hat{\beta}$ to represent the traits of the mutant strain. If we were to draw up the dynamics for $d\hat{S}/dt$ and $d\hat{I}/dt$ of the mutant population, the invasion part of the Jacobian matrix, evaluated at the resident-only equilibrium, would be

$$\begin{pmatrix} \hat{a} - qH - b - \hat{\beta}I - cP & \hat{a} - qH + \gamma \\ \hat{\beta}I & -\Gamma - c\phi P \end{pmatrix}, \tag{3}$$

where $\Gamma = \alpha + b + \gamma$. The fitness is given by the maximum eigenvalue of this matrix (Metz *et al.*, 1996a; Geritz *et al.*, 1998), although we can derive a sign equivalent form of the fitness, which we hereafter call the fitness for convenience, as the negative of the determinant of this matrix (see Appendix A for proof), i.e.

$$s(\hat{a}, \hat{\beta}; a, \beta) = (\hat{a} - qH - b - \hat{\beta}I - cP)(\Gamma + c\phi P) + \hat{\beta}I(\hat{a} - qH + \gamma). \tag{4}$$

(We have not yet included the trade-off.) We use the method of trade-off and invasion plots to analyse the evolutionary behaviour. Here we calculate two invasion boundaries: the $f_1$ invasion boundary, of the form $\hat{a} = f_1(\hat{\beta}, \beta)$ derived from $s(\hat{a}, \hat{\beta}; a, \beta) = 0$ (taking $a = f(\beta)$), which separates the $(\hat{a}, \hat{\beta})$-space into regions where a mutant with traits $(\hat{a}, \hat{\beta})$ can and cannot invade a resident with traits $(a, \beta)$, and the $f_2$ invasion boundary, of the form $\hat{a} = f_2(\hat{\beta}, \beta)$, derived from $s(a, \beta; \hat{a}, \hat{\beta}) = 0$ (again taking $a = f(\beta)$), which separates the $(\hat{a}, \hat{\beta})$-space into regions where a mutant with traits $(a, \beta)$ can and cannot invade a resident with traits $(\hat{a}, \hat{\beta})$.

An evolutionary singularity occurs when the trade-off $\hat{a} = f(\hat{\beta})$ is tangential to the invasion boundaries at the point $(\hat{a}, \hat{\beta}) = (a, \beta)$ (the two invasion boundaries are always tangential at that point). The relative curvatures of the trade-off and the two invasion boundaries, evaluated at an evolutionary singularity, determine the evolutionary properties of that singularity, in particular evolutionary stability (ES) – whether a singularity can be invaded – and convergence stability (CS) – whether species will evolve towards or away from a singularity. (See Appendix B for full details and workings.) Combinations of these determine the nature of the evolutionary singularity. It can be an evolutionary attractor (CSS) if it is ES and CS, an evolutionary branching point if it is CS but not ES, or an evolutionary repellor (in which we also include a 'Garden of Eden' point or ES-repellor) if it is not CS (the ES status is then mostly irrelevant).

In our model, it is possible for the evolutionary singularity to exhibit any of the long-term behaviour mentioned above, depending on the choice of parameter values and trade-off shape.

We find that especially interesting behaviour occurs in the model if the singularity (specifically the singularity at $\beta^* = 1$) is an evolutionary repellor, and the prey is initially below (lower $\beta$) the singular point. Here the prey evolves away from the singularity towards an extreme state of high resistance (i.e. low transmission), which will move the system towards a point where the pathogen is excluded. This exclusion (or invasion) threshold for infection (although we assume a predator-free environment, we have left $c$ in for results later) is given by

$$R_{0I} = \frac{\beta S_{XI}}{\alpha + b + \gamma + c\phi P_{XI}} = 1, \tag{5}$$

where $S_{XI}$ (and $P_{XI}$) represent the equilibrium density of the prey (and predator) in the absence of the pathogen. This threshold (along with the host extinction threshold given by $a = b$) is plotted in trade-off space in Fig. 1A. If the prey evolves to a point where the *reproduction ratio* $R_{0I}$ in (5) is less than 1, the pathogen can be excluded from the environment. (This may not be the case in more complex model set-ups where backwards bifurcations can occur; in that case, invasion and exclusion boundaries can be different. Here, however, and in all simulations throughout our study, backwards bifurcations do not occur.) However, analysis about this point of exclusion reveals some interesting conclusions.

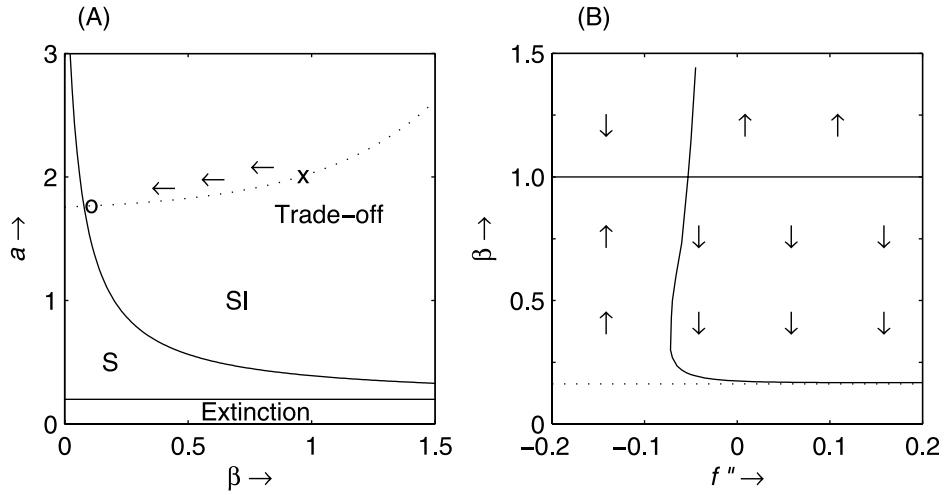


**Fig. 1.** In (A) we plot the exclusion threshold $R_{0I} = R_0 = 1$ in trade-off space. The letters in each region denote the species that would be present (have positive density): S = uninfected prey only, SI = infected co-existence. The lower extinction threshold is when the prey birth rate falls below the natural death rate. The trade-off (dashed line) corresponds to that in Fig. 2B, where 'o' denotes the CS singularity, 'x' represents repellor singularity, and the arrows the direction of evolution before pathogen exclusion. In (B) we plot the singularities $\beta^*$ for different trade-off curvatures. The dashed curve represents the exclusion threshold, and the arrows represent the direction of evolution with respect to $\beta$. The parameter values are $q = 0.5$, $b = 0.2$, $\alpha = 0.2$, $\gamma = 0.2$, $c = 0$, $\theta = 1$, $d = 0.3$, $\phi = 3$.

It is clear that in the absence of infection the prey will evolve to maximize the birth rate $a$, since the cost of a higher infection rate, $\beta$, is irrelevant. We therefore have a positive fitness gradient when $I = 0$. In contrast, if – with infection present – the prey evolves higher resistance (lower $\beta$), and correspondingly a lower birth rate, then the fitness gradient is negative. Hence there must be a change of sign in this fitness gradient near (just above) the exclusion boundary. Consequently, this change in sign means a singularity must be present before the exclusion boundary is reached; furthermore, given the sign of the fitness gradient either side, we conclude this singularity must be convergent stable (CS) (i.e. an evolutionary attractor or branching point). We can confirm this by plotting the location of the singularities as we vary the trade-off curvature via $f''(1)$ (Fig. 1B). Given a trade-off with an appropriate curvature, the singularity near the exclusion boundary can be a branching point. A numerical simulation for this is shown in Fig. 2A. (See Appendix C for details of how these simulations were carried out.) Here the prey evolves higher resistance, to a point where $\beta$ is close to the exclusion boundary. The singularity, which is CS but not ES, then causes the population to branch and the two branches to evolve away from each other. Although one branch has passed beyond the exclusion boundary, the presence of the other strain (with increasing $\beta$) maintains the infection.

It is interesting to note that the lower singularity asymptotes towards the exclusion boundary, getting closer as the trade-off curvature becomes larger (Fig. 1B). Theoretically, according to adaptive dynamics, this protects the pathogen from ever being excluded from the system because, assuming small, rare mutations, selection cannot drive the population across the exclusion boundary and the infected population to zero (although, when the singularity is near the boundary, the pathogen will exist only at very low levels). This initially occurs in our numerical simulations in Fig. 2B (and subsequent figures later in the paper). Here we plot the evolution of $\beta$ given that the evolutionary singularity at $\beta^* = 1$ is a repellor. Initially, $\beta$ evolves away from the singularity and towards the lower singularity just above the exclusion threshold (Fig. 2B). As this is an attractor, it 'stops' here, near this singularity. However, this is temporary, the simulations then go on to exhibit further evolutionary behaviour. In the more realistic case where mutations are not arbitrarily small, when the singular point is sufficiently near the threshold, a mutant that does not itself support the pathogen can arise. This resistant strain cannot remove the pathogen from the system deterministically (it cannot truly invade in the sense of adaptive dynamics). However, its presence suppresses the infection further, essentially to negligible levels, and we find it can take the resident a very long time to out-compete this mutant strain; hence a strain below the threshold is temporarily present in our simulations in Fig. 2B. During this time, the infection levels continue to fall due to the presence of these resistant mutants below the threshold. We recognize that stochastic effects occur in nature and correspondingly employ them in our simulations. Thus as the infection falls, it becomes prone to stochastic extinction. The simulations therefore deviate from adaptive dynamics theory; they incorporate the fact that at low levels the infection (and in fact any population component with low enough density) has a high probability of extinction. Here we indeed find that the infection reaches such negligible levels for a sustained period of time and may easily be driven to extinction by stochastic effects, and as such it is removed from the simulations (Fig. 2C). Of course, the probability of this extinction is much enhanced by the fact that the lower singularity is near the exclusion threshold and supports only a very low level of infection. After extinction of the pathogen, any benefit – through higher resistance – the mutant has will be lost and subsequent mutants that arise will be uninfected and a new

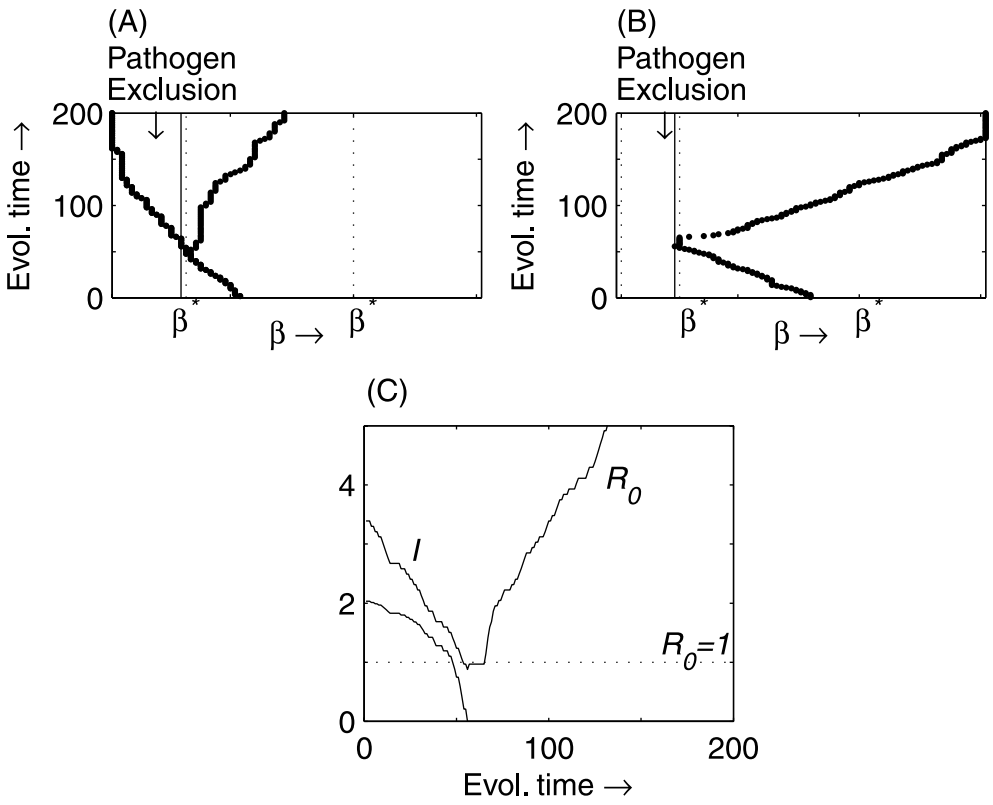


**Fig. 2.** (A, B) Numerical simulations of the evolution of $\beta$ with a trade-off of the form $a = f(\beta)$, from (2), where $f''(1) = -0.05$ in (A) and $f''(1) = 1.25$ in (B), both giving rise to an evolutionary repellor at $\beta^* = 1$. Here $\beta$ evolves away from this singularity and towards the singularity just above the exclusion threshold. In (A) this singularity is a branching point and in (B) it is an attractor. In (B) it temporarily settles at the lower singularity, although random (non-negligible) mutations take $\beta$ across the threshold. When it crosses the pathogen exclusion threshold, the infected prey density drops to zero. (See end of Section 3 for full details.) (C) Plot of the infected equilibrium density $I$ and the reproduction ratio $R_0$ ($R_{0I}$ with $c = 0$), as given in (5), at each evolutionary step are for the simulation shown in (B). The infected density, $I$, reaches negligible levels when the reproduction ratio falls below 1, and is subsequently in danger of extinction. Due to the exclusion of the pathogen, and hence the change in selection pressure, $\beta$ now increases to the upper limit so as to maximize reproduction $a$. The parameter values are $q = 0.5$, $b = 0.2$, $\alpha = 0.4$, $\gamma = 0.2$, $c = 0$, $f'(1) = 0.078$.

evolutionary path will be followed, with $S = S_{XI}$ and $I = 0$. The prey evolves to maximize the birth rate $a$ without encountering any further singularities ($\beta$, which is also maximized, only affects the fitness via the trade-off and is not selected upon). However, since at these higher transmission rates the population dynamic equilibria are such that $R_0 > 1$, the prey will be vulnerable to future outbreaks by the pathogen and to returning to the endemic state.

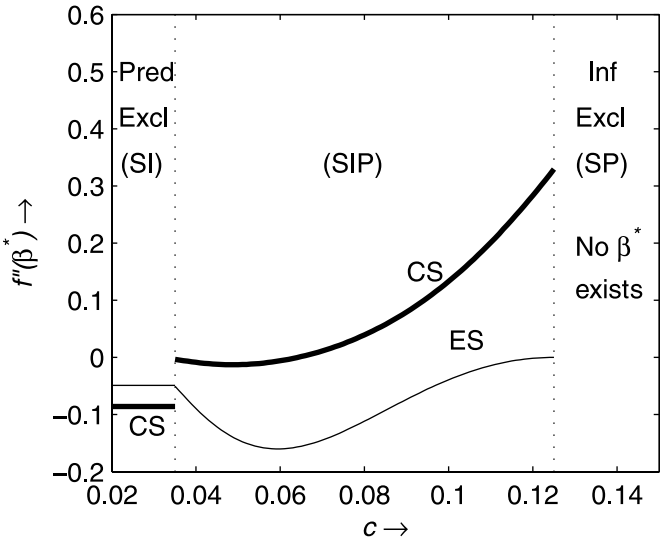


**Fig. 3.** The trade-off curvature $f''(1)$ needed to satisfy ES (thin line) and CS (thick line) conditions, for the singularity at $\beta^* = 1$ (where below each boundary corresponds to satisfying the relevant property) for a range of values of $c$. Below both lines denotes an attractor, above the CS line a repellor, and between the two (when the CS line is above the ES line) a branching point. The letters in brackets denote the species that is present: S = susceptible prey, I = infected prey, and P = predator. The parameter values are $q = 0.5$, $b = 0.2$, $\alpha = 0.2$, $\gamma = 0.2$, $a^* = 2$, $\beta^* = 1$, $\theta = 1$, $d = 0.3$, $\phi = 3$.

## 4. EVOLUTION OF RESISTANCE IN THE PRESENCE OF A (NON-EVOLVING) PREDATOR

### 4.1. Evolutionary effects of the predator

We again consider a trade-off between the transmission rate, $\beta$, and the birth rate, $a$, although we now assume a predator is present and take $c > 0$ in (1). The fitness is that in (4). The introduction of the predator immediately increases the dimension of the feedback environment. Consequently, this can produce significant shifts in evolutionary behaviour such that a singularity that was a repellor (non-CS) can become convergent stable (an attractor or branching point) without the need to change any other parameter values or trade-off. In Fig. 3 we plot the boundaries for the ES and CS properties, in terms of the trade-off curvature at the singularity at $\beta^* = 1$, as we vary the rate of predation. If $c$ is too low, the predator is excluded from the environment, and the system returns to that in the previous section, but if $c$ is too high, the pathogen is excluded, in which case the prey maximize their birth rate as there is no cost in terms of a lower resistance. However, for intermediate values of $c$, where the prey, pathogen, and predator co-exist, the general trend is that the size of the branching region between the two boundaries (by size we mean range of values of the trade-off curvature which produce a branching point) increases as $c$ increases.

We briefly draw attention to the discontinuity in the CS boundary during the transition from a predator-free environment to a predator–prey–infection environment in Fig. 3. This discontinuity is caused by the way the population densities at the demographic attractor

(equilibrum) change through the transition. Although this is continuous (e.g. $P$ goes towards zero as $c$ passes (decreases) through the transition), it is not smooth. This results in a discontinuity in the gradient of the densities at the attractor, i.e. in $\partial S/\partial\beta$, $\partial I/\partial\beta$, and $\partial P/\partial\beta$ – this can be seen by the difference in $\partial S/\partial\beta$ through this point as shown in equation (D1); similar differences are present in the $I$ and $P$ derivatives. This in turn causes a discontinuity in the CS boundary as this depends on the mixed derivative $\partial^2 s/\partial\beta\partial\hat{\beta}$, which in turn depends on the above gradients. Conversely, the ES boundary is continuous but not smooth, as this depends only on the densities (which are continuous but not smooth) and not on their gradients. (See Hoyle *et al.* (2011), who explain this behaviour for a discrete time system in more detail.)

### 4.2. Predator and pathogen exclusion thresholds

Critically in this system there exists not only a pathogen exclusion threshold, as given by equation (5) (where $c$ is non-zero now), but also a predator exclusion threshold. This bounds a parameter region where the predator cannot survive. For our model (1), this is given by

$$R_{0P} = \frac{\theta c}{d}(S_{XP} + \phi I_{XP}) = 1, \tag{6}$$

where $S_{XP}$ and $I_{XP}$ represent the equilibrium densities of the prey in the absence of the predator. This is equivalent to the requirement that the number of offspring a single predator would produce over its lifetime in an entirely prey environment – equivalent to the reproduction number – needs to be greater than 1 for the predator to establish. If evolution were to drive this predator ratio below 1, the predator could not survive and would be driven extinct. (Again backwards bifurcations do not occur here and so invasion and exclusion boundaries are equivalent.) Subsequent evolution of resistance by the prey would be determined in the predator-free environment (as $P$ would remain zero), and hence as discussed in Section 3.

Thresholds for when the predator and pathogen will be excluded under different scenarios can be derived. Combining these we can plot these thresholds in trade-off space. (We note that these boundaries are independent of the explicit functional form of the trade-off.) Figure 4 shows two examples, for primarily different values of $\phi$ (the change in the predation due to prey being infected). In Fig. 4A, with $\phi = 3$ (i.e. infectious prey are more vulnerable to predation), the trade-off intersects three separate regions; starting in a predator–prey–infection environment, moving down the trade-off, in the direction of higher resistance (lower $\beta$), first leads to the exclusion of the predator and later the exclusion of the pathogen. In Fig. 4B, with $\phi = 0.8$ (i.e. infectious prey are less vulnerable to predation), gaining higher resistance (moving down the trade-off) will lead to the exclusion of the pathogen but not the predator. In general, whether the pathogen or predator is excluded first (or at all) depends on which ratio, $R_{0P}$ or $R_{0I}$, falls below 1 first, with each of them depending on a range of parameters.

Numerical simulations of the evolution of resistance for the case where the singularity at $\beta^* = 1$ is an evolutionary repellor are shown in Fig. 5, where we focus on the situation described in Fig. 4A.

First, we focus on Figs. 5A–D. Here the singularity leads $\beta$ to evolve to the lower extreme value. However, there is a CS singularity at the threshold, now protecting the predator from

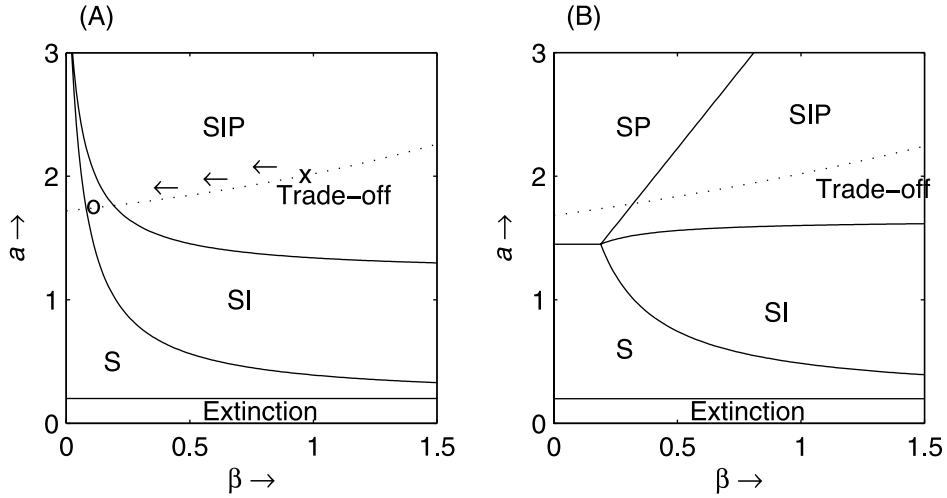


**Fig. 4.** Two plots of the exclusion boundaries given in (5) and (6) in trade-off space, with a trade-off between the prey reproduction rate and infection rate, $a = f(\beta)$ (with $f''(1) = 1.25$). The dashed line in (A) represents a given trade-off used in Figs. 5E–H. We plot an equivalent trade-off in (B) just for comparison. The letters in each region denote the species that would be present (have positive density). S = uninfected prey only, SI = infected prey, SIP = infected prey and predator, SP = uninfected prey and predator. [Assumes we start from an SIP (S > 0, I > 0, P > 0) environment.] The parameter values are $q = 0.5$, $b = 0.2$, $\alpha = 0.2$, $\gamma = 0.2$, $c = 0.05$ in (A), $c = 0.12$ in (B), $\theta = 1$, $d = 0.3$, $\phi = 3$ in (A), $\phi = 0.8$ in (B), $f'(1) = 0.0935$ in (A) and $f'(1) = 0.0345$ in (B).

exclusion (Fig. 5D). This singularity in fact asymptotes towards the predator exclusion boundary but will never cross it. The reason for this lies in the fact that here $\alpha = 0$. Hence, when the predator is excluded, there is no cost in the prey being infected (as there is no castration, no increased death rate and, with the predator excluded, no change in predation). Therefore, the prey will evolve to maximize its birth rate, with a higher $\beta$ giving no cost (i.e. it will have a positive fitness gradient). This positive fitness gradient below the threshold prevents the singularity from ever passing the threshold (similar to the pathogen exclusion case). However, once the prey reaches the singularity at the threshold, the predator will only exist at very low numbers at this singularity, with the predator ratio, $R_{0P}$ in (6), lying just above 1. Here a combination of non-arbitrarily small mutations and the exclusion of strains at very low density will again lead to the extinction of the predator (as in the case of the pathogen at the end of Section 3) (Fig. 5C). After this point, the change in selection pressure mentioned above causes $\beta$ to increase and the infection is maintained in the environment. Again, it should be noted that this leaves the prey vulnerable to future predator invasions.

In contrast, in Figs. 5E–H, with a small change in $\alpha$ from 0 to 0.2 (i.e. an increase in the pathogen-induced death rate), the lower singularity can now, and does, pass below the predator exclusion threshold (Fig. 5H) and in this case asymptotes towards the pathogen exclusion threshold. Here the predator will inevitably be excluded deterministically (this can occur with the standard small, rare mutations of adaptive dynamics). The situation changes such that once the prey has crossed the predator exclusion boundary, and the predator is excluded, the prey continues to evolve in a way that leads $\beta$ to decrease and the infection

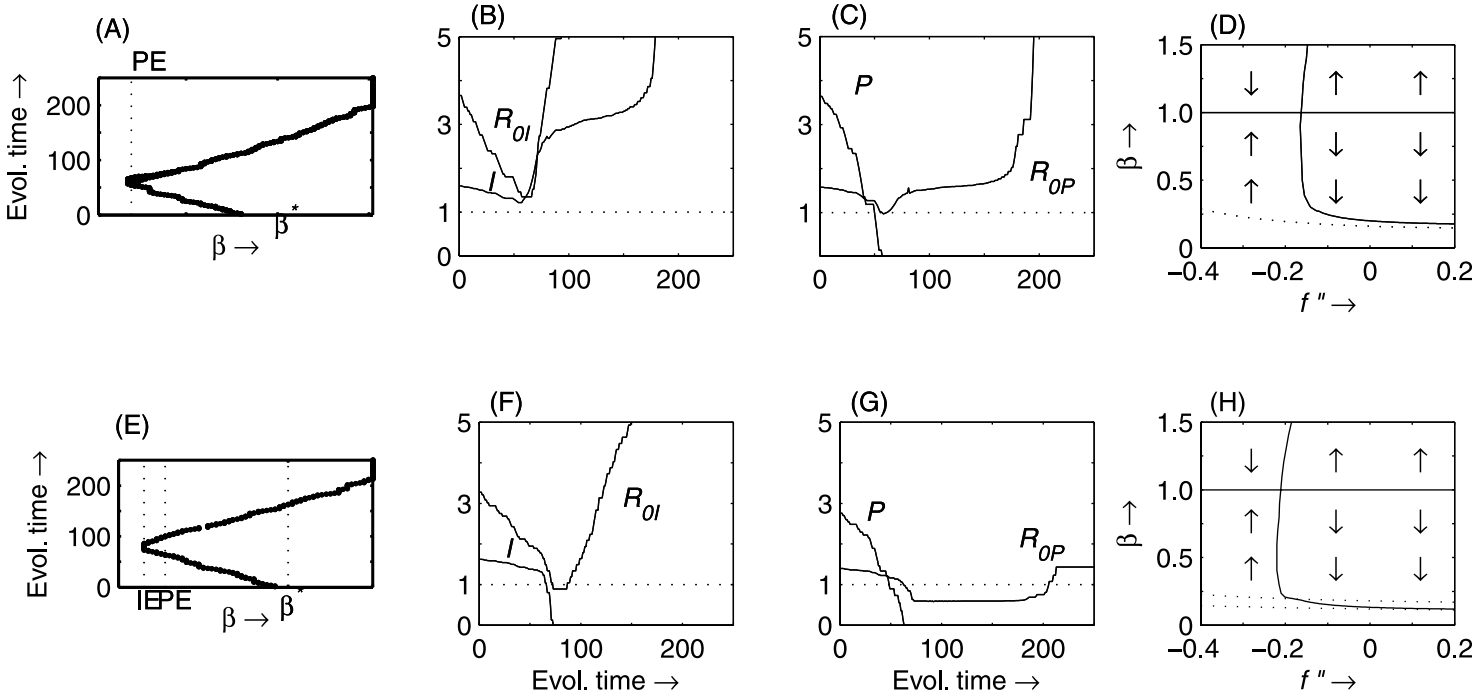


**Fig. 5.** Numerical simulations of the evolution of $\beta$ with a trade-off of the form $a = f(\beta)$ (from (2)) with $f''(1) = 1.25$. Here the singularity at $\beta^* = 1$ is an evolutionary repellor. These simulations are run for two values of the pathogen-induced death rate $\alpha$: 0 in (A–D) and 0.2 in (E–H). In (A) and (E) we show the evolution of $\beta$, where IE = infection exclusion threshold and PE = predator exclusion threshold. In (B) and (F) we plot the infection density $I$ at each evolutionary time step along with the ratio $R_{0I}$, as given in equation (4). In (C) and (G) we plot the predator density $P$ at each evolutionary time step along with the ratio $R_{0P}$, as given in equation (6). In each case, a ratio below 1 leads to the extinction of the infection or predator. In (D) and (H) we plot the location of the evolutionary singularities for various shapes of trade-off. The dashed line represents the predator exclusion boundary $R_{0P} = 1$, as given in equation (6), and the lower dashed line in (H) represents the infection threshold $R_{0I} = 1$. The parameter values are $q = 0.5$, $b = 0.2$, $\gamma = 0.2$, $c = 0.05$, $\theta = 1$, $d = 0.3$, $\phi = 3$, $f'(1) = 0.0935$ in (A–D) and $f'(1) = 0.114$ in (E–H).

is subsequently excluded as the prey crosses the infection exclusion threshold in the manner described previously (Figs. 5E–H). After this point, the infection-free environment changes the selection pressure such that higher $\beta$ comes at no cost and the prey subsequently evolves to maximize the birth rate $a$. Again this leaves the prey vulnerable to future invasion from both the predator and the pathogen.

## 5. CO-EVOLUTION OF PREY AND PREDATOR

We now expand on the situation above, where the prey evolves in such a way to drive the predator to extinction (Fig. 5); we now let the predator evolve too and investigate whether this co-evolutionary set-up allows the predator to survive. We focus on the situation (Figs. 5A–D) where the prey evolved to decrease $\beta$, which eventually excluded the predator and an infected prey-only system remained; this is the only case we consider here.

We take the predation rate, $c$, and predator death rate, $d$, to evolve and suppose that they are linked by a trade-off of the form $d = g(c)$. The fitness of a rare mutant predator, with traits $(\hat{c}, \hat{d})$, attempting to invade an established resident, with traits $(c, d)$, in a stable equilibrium with densities $S$, $I$, $P$, where the prey has traits $(\alpha, \beta)$, is given by

$$r(\hat{c}, \hat{d}; c, d, a, \beta) = \theta\, \hat{c}(S + \phi I) - \hat{d}. \tag{7}$$

[Correspondingly, the fitness of (4) is now best denoted $s(\hat{a}, \hat{\beta}; a, \beta, c, d)$.] Under this model and trade-off, the predator's evolutionary behaviour follows that of an optimization set-up, whereby $(S + \phi I)$ is minimized, and subsequently any singularity is an evolutionary attractor for acceleratingly costly trade-offs, or an evolutionary repellor for deceleratingly costly trade-offs – branching points are not possible. [For further details on this, and the repercussions of a one-dimensional feedback environment, see Metz *et al.* (1996b), Heino *et al.* (1998), Kisdi (1998), Rueffler *et al.* (2006), and Hoyle and Bowers (2008).]

By allowing the prey and predator to co-evolve, we show, via numerical simulations, that the predator can indeed prevent its own extinction. In particular, we initially assume that the predator has a higher per capita mutation rate than the prey (with a ratio of 3:1), potentially allowing the predator to evolve 'faster' than the prey. As $\beta$ decreases (Fig. 6A), given an appropriate trade-off, $c$ increases (Fig. 6B). This moves the predator exclusion threshold (6) (and Fig. 4) in such a way that it moves below the pathogen exclusion threshold, and therefore as $\beta$ decreases the pathogen threshold is met first and the pathogen is excluded (Fig. 6C). Again there will exist a singularity just above the pathogen threshold, although sufficiently large mutations again lead to $\beta$ crossing the exclusion threshold with $I$ becoming negligible and the pathogen becoming extinct. In Fig. 6D we plot the predator density and the ratio $R_{0P}$ at evolutionary time steps, which remain above 0 and 1 respectively at all times. However, the possibility of the above occurring depends on the predator's optimal evolutionary strategy, which subsequently optimizes $(S + \phi I)$ to be in a region that allows predator survival; if this is not the case, the predator cannot survive no matter how fast it evolves.

In Figs. 6E–H, we plot equivalent results, although in this case we set the per capita mutation rates of the predator and prey to be equal, such that it would take longer (than previously) for the predator to decrease its exclusion threshold to a 'safe' level to prevent its own extinction. Here the predator does not evolve enough and the predator exclusion threshold remains above the prey exclusion threshold. In this case, the prey evolves to such a level that $\beta$ crosses the predator exclusion threshold and the predator is driven extinct.

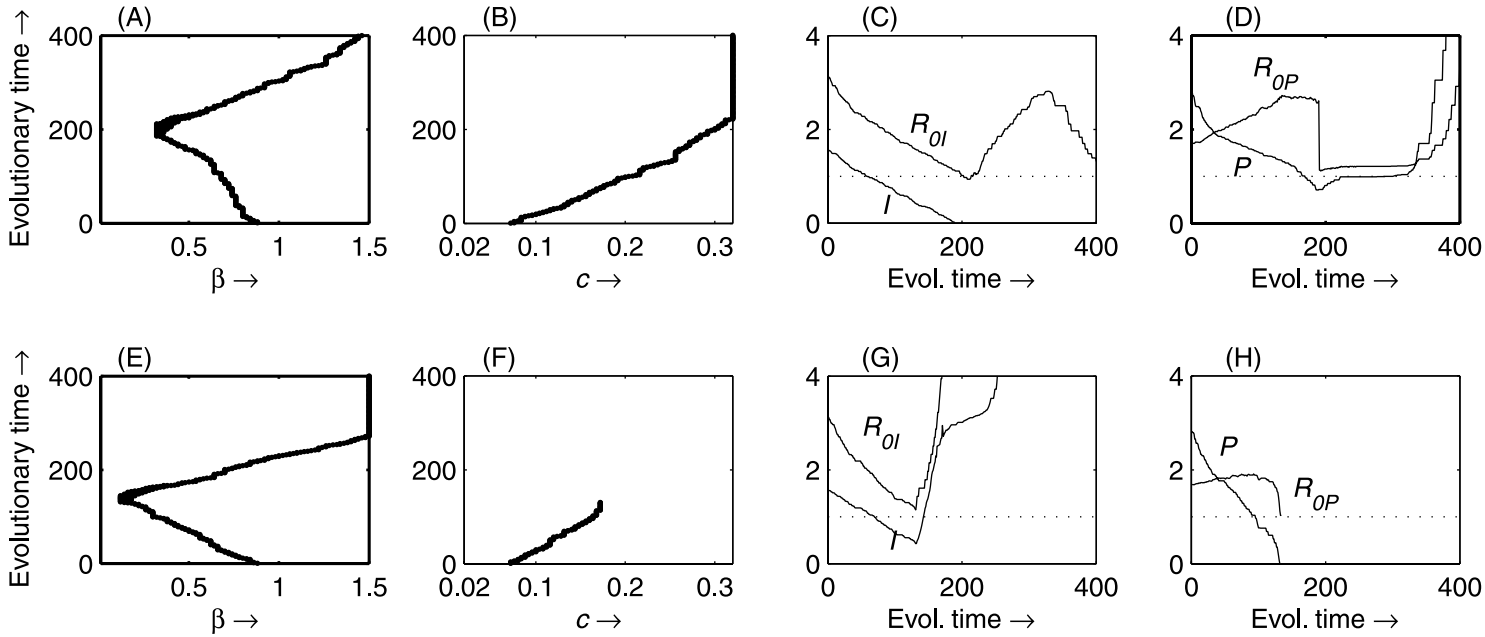


**Fig. 6.** Numerical simulations of the evolution of $\beta$ for the prey, with a trade-off of the form $a = f(\beta)$, with $f''(1) = 1.25$, and of $c$ for the predator, with a trade-off of the form $d = g(c)$, with $g''(0.05) = -5$ (which we take to have an equivalent form to that for the prey in (2) with $c^* = 0.05$ and $d = 0.3$). Evolution is such that the prey evolves to minimize $\beta$ and the predator evolves to maximize $c$. In (A) and (B) the predator manages to keep its ratio $R_{0P}$ above 1 to allow it to co-exist with the prey (D); however, the pathogen is excluded as its ratio $R_{0I}$ drops below 1 (C). In (E) and (F) the predator is not able to keep its ratio above 1 and therefore the predator is driven extinct (H); however, the pathogen remains in the environment (G). The parameter values are $q = 0.5$, $b = 0.2$, $\alpha = 0.2$, $\gamma = 0.2$, $\theta = 1$, $\phi = 3$, $f'(1) = 0.0935$, $g'(0.05) = 6$.

Again there will exist a singularity very close to the threshold, although appropriate mutations again lead to the crossing of this threshold and the extinction of the predator. As was the case in Figs. 5A–D, once the predator has been excluded, the system remains in a prey–infection set-up and the prey evolves to maximize $\beta$, and subsequently its birth rate, as there is no cost in the prey being infected (as there is no castration and no increased death rate, as $\alpha = 0$).

## 6. DISCUSSION

It is well known that for pathogens to invade and persist commonly requires the host population size to be above a certain threshold, which can generally be derived from the pathogen's reproduction ratio $R_0 = 1$ (Anderson and May, 1981; Bremermann and Pickering, 1983; Bremermann and Thieme, 1989). In models where pathogen invasion thresholds and exclusion thresholds are coincident, which is the case here, this reproduction ratio can be used to determine the conditions needed for a pathogen to be excluded from a host population. Of interest here is the important problem concerning the conditions under which a host species can evolve in such a way that it falls below this threshold. In the present work, it is seen that evolving greater resistance (at a cost of lowered fecundity) is not sufficient under standard adaptive dynamics analysis (with small, rare mutations) to achieve a state where the population size falls below a level corresponding to $R_0 = 1$; there is a protective CS singularity preventing this. However, when this singularity is also ES and is sufficiently close to the exclusion boundary, in the realistic case where the mutations are not arbitrarily small, this protection may fail. A mutant that does not itself support the pathogen can arise. Furthermore, this strain can suppress the density of infected hosts to sufficiently low levels that the infection may be lost due to stochastic effects at low population numbers. Subsequently, new mutants that arise will be uninfected and a new evolutionary path will be followed. Such behaviour is seen in the simulations presented here.

However, as in most previous studies, this result assumes an environment populated by the host and pathogen only, with secondary species/interactions commonly ignored. Recently, however, studies at a population level have shown that additional interacting species can have a significant effect on the dynamics of a system (e.g. Hudson and Greenman, 1998; Greenman and Hoyle, 2010; Haque, 2010; Haque and Greenhalgh, 2010; Venturino, 2010), which in turn causes complications for deriving control strategies (Greenman and Hoyle, 2010). These interactions still remain relatively ignored at an evolutionary level. Recent studies by Morozov and Adamson (2011) and Morozov and Best (2012) have tried to change this, looking at pathogen evolution in an SI model, where a predator feeds on infected prey only. They found that the addition of even a simple predator can change the evolutionary dynamics significantly. This is emphasized even more strongly in the present work where we found an example where, given specific parameter values, the presence of a predator can create the possibility of branching points where none were present previously. Significantly, the way in which the predators affect the exclusion boundaries, $R_0 = 1$ proves pivotal. Due to the predator, there are now two thresholds, $R_{0I} = 1$ (number of new infections a single infected prey can make in a completely susceptible environment) and $R_{0P} = 1$ (number of offspring a single predator can produce over its lifetime in prey-only environment), where the pathogen and the predator respectively can be excluded (can invade) from a predator–prey–infection environment.

Although these ratios depend on most of the parameters, a key factor in determining whether the pathogen or predator is excluded first is $\phi$, the change in predation experienced

by a prey when it becomes infected (Fig. 4). A high value of $\phi$, where the predator is largely dependent on infected prey for food, led to the predator being excluded first as resistance decreased the number of infected prey and hence the predator's food source; this result echoes that seen by Morozov and Adamson (2011). Subsequent evolution depends on the selection pressures in a prey-only SIS system – for example, co-existence of prey and pathogen (Figs. 5A–D) or pathogen exclusion (Figs. 5E–H). Again, we found exclusion of the parasite requires finite mutations allowing resistance levels to cross the corresponding threshold; however, exclusion of predators is found to be possible by host evolution by a parallel mechanism but also in appropriate circumstances by the standard small, rare mutations of adaptive dynamics theory. A low value of $\phi$, where the predator mostly consumes uninfected prey, led to the pathogen being excluded first as resistance drove down the number of infected prey with the predator pushing down the susceptible prey.

Generally throughout we see that if the predator is present, it can go extinct due to host evolution. In the (final) case where the predator was allowed to co-evolve, it is seen that the predator can prevent its own extinction by evolving in such a way that it lowers its threshold and allows itself to stay above the predator reproduction threshold $R_{0P} = 1$. In particular, we found that the relative per capita mutation rates of the predator and prey are key to whether the predator can persist in the population. The 'speed' of evolution in the two species depends on population sizes, mutation rates, and selection gradients (Dieckmann and Law, 1996; Marrow *et al.*, 1996), and we found that if the predator evolves significantly 'faster' than the prey due to an increased mutation rate, it was able to shift its extinction threshold sufficiently quickly to prevent the prey driving its extinction. These subtle effects of evolution require further investigation to fully understand the co-evolutionary dynamics.

A question that is often raised in these systems, especially at a population studies level, is how the behaviour would change if the pathogen could infect both prey and predator. Studies have shown that the resultant behaviour can be more complicated. One population level study by Greenman and Hoyle (2010) showed that the control maps (plots of invasion/exclusion thresholds in two-parameter space) can become ever more complicated and that exclusion boundaries can become very close together, potentially leading to multiple exclusions in quick succession. However, more detailed analysis would be needed to determine the effects of shared-pathogens in an evolutionary sense and, in particular, to investigate whether cross-species infection levels would allow for a larger potential pool of susceptibles and make the infection more difficult to exclude, which might perhaps play against the predator.

Understanding the persistence of pathogens in natural populations is key to the management of many ecological systems. We have shown here how the evolution of host resistance may drive its pathogen to extinction and how the shape of the trade-off between resistance and reproduction is crucial to this possibility. Furthermore, we have shown how this result can be complicated by the presence of an immune predator, considerably changing the evolutionary outcomes and in some cases producing opposite results to when species exist alone (e.g. CS switches to non-CS). This alone provides a reason why more studies into complex ecosystems should be carried out. The interactions of all three species can lead to relatively complex evolutionary dynamics, with the shape of the host's trade-off and the relative level of predation experienced by susceptible and infected hosts being key.

## ACKNOWLEDGEMENTS

Thanks to Éva Kisdi for some very useful comments. A.H. was supported by a Carnegie Research Grant.

## REFERENCES

Anderson, R.M. and May, R.M. 1981. The population dynamics of microparasites and their invertebrate hosts. *Phil. Trans. R. Soc. Lond. B*, **291**: 452–524.

Best, A., White, A. and Boots, M. 2009. The implications of co-evolutionary dynamics to host–parasite interactions. *Am. Nat.*, **173**: 779–791.

Best, A., White, A. and Boots, M. 2010a. Resistance is futile but tolerance can explain why parasites do not always castrate their hosts. *Evolution*, **64**: 348–357.

Best, A., White, A., Kisdi, É., Antonovics, J., Brockhurst, M. and Boots, M. 2010b. Evolution of host-parasite range. *Am. Nat.*, **176**: 63–71.

Boots, M. 2008. Fight or learn to live with the consequences? *Trends Ecol. Evol.*, **23**: 248–250.

Boots, M. and Bowers, R.G., 1999. Three mechanisms of host resistance to microparasites – avoidance, recovery and tolerance – show different evolutionary dynamics. *J. Theor. Biol.*, **201**: 13–23.

Boots, M. and Bowers, R.G., 2004. The evolution of resistance through costly acquired immunity. *Proc. R. Soc. Lond. B*, **271**: 715–723.

Boots, M. and Haraguchi, Y. 1999. The evolution of costly resistance in host–parasite systems. *Am. Nat.*, **153**: 359–370.

Boots, M., Best, A., Miller, M.R. and White, A. 2009. The role of ecological feedbacks in the evolution of host defence: what does theory tell us? *Phil. Trans. R. Soc. Lond. B*, **364**: 27–36.

Bowers, R.G., White, A., Boots, M., Geritz, S.A.H. and Kisdi, É. 2003. Evolutionary branching/speciation: contrasting results from systems with explicit or emergent carrying capacities. *Evol. Ecol. Res.*, **5**: 883–891.

Bowers, R.G., Hoyle, A., White, A. and Boots, M. 2005. The geometric theory of adaptive evolution: trade-off and invasion plots. *J. Theor. Biol.*, **233**: 363–377.

Bremermann, H.J. and Pickering, J. 1983. A game-theoretical model of parasite virulence. *J. Theor. Biol.*, **100**: 411–426.

Bremermann, H.J. and Thieme, H. 1989. A competitive exclusion principle for pathogen virulence. *J. Math. Biol.*, **27**: 179–190.

de Mazancourt, C. and Dieckmann, U. 2004. Trade-off geometries and frequency-dependent selection. *Am. Nat.*, **164**: 765–778.

Dieckmann, U. and Law, R. 1996. The dynamical theory of coevolution: a derivation from stochastic ecological processes. *J. Math. Biol.*, **34**: 579–612.

Dieckmann, U., Metz, J.A.J., Sabelis, M.W. and Sigmund, K. 2002. *Adaptive Dynamics of Infectious Diseases: In Pursuit of Virulence Management*. Cambridge: Cambridge University Press.

Eshel, I. 1983. Evolutionary and continuous stability. *J. Theor. Biol.*, **103**: 99–111.

Frank, S.A. 1993. Co-evolutionary genetics of plants and pathogens. *Evol. Ecol.*, **7**: 45–75.

Geritz, S.A.H., Kisdi, É., Meszéna, G. and Metz, J.A.J. 1998. Evolutionary singular strategies and the adaptive growth and branching of the evolutionary tree. *Evol. Ecol.*, **12**: 35–57.

Greenman, J.V. and Hoyle, A. 2010. Pathogen exclusion from eco-epidemiological systems. *Am. Nat.*, **176**: 149–158.

Haque, M. 2010. A predator–prey model with disease in the predator species only. *Nonlinear Analysis: Real World Applications*, **11**: 2224–2236.

Haque, M. and Greenhalgh, D. 2010. When a predator avoids infected prey: a model based theoretical study. *Math. Med. Biol.*, **27**: 75–94.

Haque, M., Zhen, J. and Venturino, E. 2009. An epidemiological predator–prey model with standard disease incidence. *Math. Methods Appl. Sci.*, **32**: 875–898.

Heino, M., Metz, J.A.J. and Kaitala, V. 1998. The enigma of frequency-dependent selection. *Trends Ecol. Evol.*, **13**: 367–370.

Hoyle, A. and Bowers, R.G. 2008. Can possible evolutionary outcomes be determined directly from the population dynamics? *Theor. Pop. Biol.*, **74**: 311–323.

Hoyle, A., Bowers, R.G., White, A. and Boots, M. 2008. The influence of trade-off shape on evolutionary behaviour in classical ecological scenarios. *J. Theor. Biol.*, **250**: 498–511.

Hoyle, A., Bowers, R.G. and White, A. 2011. Evolutionary behaviour, trade-offs and cyclic and chaotic population dynamics. *Bull. Math. Biol.*, **73**: 1154–1169.

Hudson, P. and Greenman, J. 1998. Competition mediated by parasites: biological and theoretical progress. *Trends Ecol. Evol.*, **13**: 387–390.

Kisdi, É. 1998. Frequency dependence versus optimization. *Trends Ecol. Evol.*, **13**: 508.

Kisdi, É. 1999. Evolutionary branching under asymmetric competition. *J. Theor. Biol.*, **197**: 149–162.

Levin, S. and Pimental, D. 1981. Selection of intermediate rates of increase in host–parasite systems. *Am. Nat.*, **117**: 308–315.

Marrow, P., Dieckmann, U. and Law, R. 1996. Evolutionary dynamics of predator–prey systems: an ecological perspective. *J. Math. Biol.*, **34**: 556–578.

Maynard Smith, J. and Price, G.R. 1973. The logic of animal conflict. *Nature*, **246**: 15–18.

Metz, J.A.J., Geritz, S.A.H., Meszéna, G., Jacobs, F.J.A. and Van Heerwaarden, J.S. 1996a. Adaptive dynamics: a geometrical study of the consequences of nearly faithful reproduction. In *Stochastic and Spatial Structures of Dynamical Systems* (S.J. Van Strien and S.M. Verduyn Lunel, eds.), pp. 183–231. Amsterdam: Elsevier.

Metz, J.A.J., Mylius, S.D. and Diekmann, O. 1996b. When does evolution optimise? On the relation between types of density dependence and evolutionarily stable life history parameters. IIASA Working Paper WP-96-004. Available at: http://www.iiasa.ac.at/Research/ADN/Series.html.

Miller, M.R., White, A. and Boots, M. 2005. The evolution of host resistance: tolerance versus control. *J. Theor. Biol.*, **236**: 198–207.

Morozov, A. and Adamson, M.W. 2011. Evolution of virulence driven by predator–prey interaction: possible consequences for population dynamics. *J. Theor. Biol.*, **276**: 181–191.

Morozov, A. and Best, A. 2012. Predation on infected host promotes evolutionary branching of virulence and pathogens' biodiversity. *J. Theor. Biol.*, **307**: 29–36.

Pugliese, A. 2002. On the evolutionary co-existence of parasite strains. *Math. Biosci.*, **177/178**: 355–375.

Restif, O. and Koella, J.C. 2003. Shared control of epidemiological traits in a co-evolutionary model of host–parasite interactions. *Am. Nat.*, **161**: 827–836.

Roy, B.A. and Kirchner, J.W. 2000. Evolutionary dynamics of pathogen resistance and tolerance. *Evolution*, **54**: 51–63.

Rueffler, C., Van Dooren, T.J.M. and Metz, J.A.J. 2004. Adaptive walks on changing landscapes: Levins' approach extended. *Theor. Pop. Biol.*, **65**: 165–178.

Rueffler, C., Van Dooren, T.J.M. and Metz, J.A.J. 2006. The evolution of resource specialization through frequency-dependent and frequency-independent mechanisms. *Am. Nat.*, **167**: 81–93.

Svennungsen, T. and Kisdi, É. 2009. Evolutionary branching of virulence in a single-infection model. *J. Theor. Biol.*, **257**: 408–418.

van Baalen, M. 1998. Co-evolution of recovery ability and virulence. *Proc. R. Soc. Lond. B*, **265**: 317–325.

Venturino, E. 2001. The effects of diseases on competing species. *Math. Biosci.*, **174**: 111–131.

Venturino, E. 2002. Epidemics in predator–prey models: disease in the predators. *IMA J. Math. Appl. Med. Biol.*, **19**: 185–205.

Venturino, E. 2010. Eco-epidemic models with disease incubation and selective hunting. *J. Comp. App. Math.*, **234**: 2883–2901.

## APPENDIX A: SIGN EQUIVALENT FORM OF THE FITNESS

The invasion matrix for the mutant is given by:

$$\begin{pmatrix} \hat{a} - qH - b - \hat{\beta}I - cP & \hat{a} - qH + \gamma \\ \hat{\beta}I & -\Gamma - c\phi P \end{pmatrix} = \begin{pmatrix} A & B \\ C & D \end{pmatrix}, \tag{A1}$$

where $B > 0$ (as $a > qH$), $C > 0$, and $D < 0$; the sign of $A$ is unknown. The eigenvalues of the invasion matrix are given by:

$$\lambda^+, \lambda^- = 0.5\left[A + D \pm \sqrt{(A+D)^2 - 4(AD - BC)}\right] = 0.5\left[A + D \pm \sqrt{(A-D)^2 + 4BC}\right], \tag{A2}$$

where the superscript on $\lambda$ represents the sign taken in solution. The discriminant of these is positive and hence we always have two real eigenvalues.

As $D < 0$, it follows that if $A < 0$, then $\lambda^- < 0$; if $A \geq 0$, it follows that $|A + D| \leq |A - D|$ and therefore that $\lambda^- < 0$. Hence the $\lambda^-$ eigenvalue will always be negative. In addition, it is trivial to show that the other eigenvalue is always larger, i.e. $\lambda^- < \lambda^+$. Therefore, we can say that the eigenvalue $\lambda^+$ is the maximum eigenvalue and subsequently the fitness of the invading mutant, which we call $s$.

As $\lambda^- < 0$, we have two options:

1. Non-invasion: $s = \lambda^+ < 0$ and therefore det $= \lambda^- \lambda^+ > 0$;
2. Invasion: $s = \lambda^+ > 0$ and therefore det $= \lambda^- \lambda^+ < 0$.

Hence the negative of the determinant is sign equivalent to the fitness, $s = \lambda^+$.

## APPENDIX B: TRADE-OFF AND INVASION PLOTS (TIPs)

The method used in this study is a geometric adaptation of adaptive dynamics, namely that of trade-off and invasion plots (TIPs) (Bowers *et al.*, 2005). Alternative geometric methods to adaptive dynamics exist (de Mazancourt and Dieckmann, 2004; Rueffler *et al.*, 2004). The advantage of all of these is that the trade-off is kept at the forefront, something that is of great interest in this work.

This method takes the fitness $s(\hat{a}, \hat{\beta}; a, \beta)$ (as given in equation 4) of a rare mutant strain with evolving traits $(\hat{a}, \hat{\beta})$ faced with a resident with traits $(a, \beta)$. The invasion boundary $\hat{a} = f_1(\hat{\beta}, \beta)$, between where the mutant can and cannot invade the resident, is determined by $s(\hat{a}, \hat{\beta}; a, \beta) = 0$ (taking $a = f(\beta)$) and here is given by

$$f_1(\hat{\beta}, \beta) = qH + \frac{(b + cP)(\Gamma + \phi cP) + \hat{\beta}I(b + \alpha + c\phi P)}{\Gamma + c\phi P + \hat{\beta}I}. \tag{B1}$$

A second invasion boundary, $\hat{a} = f_2(\hat{\beta}, \beta)$, can be gained by solving $s(a, \beta; \hat{a}, \hat{\beta}) = 0$, where the roles of the mutant and resident are reversed. We do not need the explicit form for this at present. These two curves are plotted in $(\hat{a}, \hat{\beta})$-space, where $(a, \beta)$ represents a special point hereby known as an origin. These invasion boundaries are coincident and tangential at the point $(\hat{a}, \hat{\beta}) = (a, \beta)$.

The third curve on a TIP is the trade-off curve, $\hat{a} = f(\hat{\beta})$. Evolutionary steps result from constructing TIPs for varying residents on $f$. For certain $\beta$, the trade-off is also tangential to

the invasion boundaries; these $\beta$ are the evolutionary singularities, $\beta^*$. For our model, differentiating (B1) with respect to $\hat{\beta}$ gives

$$\frac{\partial f_1}{\partial \hat{\beta}} = \frac{I(\Gamma + c\phi P)(cP(\phi - 1) + \alpha)}{[\Gamma + c\phi P + \hat{\beta} I]}. \tag{B2}$$

Using the fact that $f'(\beta)$ is tangential to the invasion boundary at $\hat{\beta} = \beta = \beta^*$, from (B2), and the equilibrium result $\beta S = \Gamma + c\phi P$, we have

$$f'(\beta^*) = \left.\frac{\partial f_1}{\partial \hat{\beta}}\right|_{\beta^*} \Leftrightarrow f'(\beta^*) = \frac{S^* I^* (cP^*(\phi - 1) + \alpha)}{\beta^* H^{*2}}. \tag{B3}$$

To determine the nature of an evolutionary singularity, we use the relative curvatures (or shapes) of the three curves at a singularity. The invasion boundaries determine which types of evolutionary singularities are possible and the trade-off determines which actually occurs.

To determine the evolutionary stability or ES boundary (Maynard Smith and Price, 1973), we require the locally possible mutants – those on the trade-off – to be on the appropriate side of the ES (invasion) boundary $f_1$. Differentiating (B2) with respect to $\hat{\beta}$, evaluating at a singularity $\hat{\beta} = \beta = \beta^*$ and using $\beta S = \Gamma + c\phi P$, gives the right-hand side of (A4) and hence the ES condition as

$$ES \Leftrightarrow \lambda f''(\beta^*) < \lambda \left.\frac{\partial^2 f_1}{\partial \hat{\beta}^2}\right|_{\hat{\beta} = \beta = \beta^*} \Rightarrow f''(\beta^*) < -\frac{2S^* I^{*2} (cP^*(\phi - 1) + \alpha)}{\beta^{*2} H^{*3}}, \tag{B4}$$

where $\lambda = sign(\partial s(\hat{a}, \hat{\beta}; a, \beta)/\partial \hat{a}\big|_{\beta^*}) = 1$ in our examples.

To determine whether the singularity is convergent stable or CS (Eshel, 1983), we need to ensure that the species evolves towards the singularity. The boundary for this is gained by constructing a fourth curve by taking the mean coordinates of $f_1$ and $f_2$ at each value of $\hat{\beta}$. At the evolutionary singularity this curve has the same gradient as $f_1$ and $f_2$; furthermore, its curvature is the mean of that of $f_1$ and $f_2$ (Bowers *et al.*, 2005). Hence to be CS the mutants must be on the appropriate side of the boundary and therefore

$$CS \Leftrightarrow \lambda f''(\beta^*) < \left.\frac{\lambda}{2}\left(\frac{\partial^2 f_1}{\partial \hat{\beta}^2} + \frac{\partial^2 f_2}{\partial \hat{\beta}^2}\right)\right|_{\hat{\beta} = \beta = \beta^*}. \tag{B5}$$

The curvature of the $f_2$ boundary at a singularity can be calculated using the curvature of $f_1$ and the mixed derivative of $f_1$ (Bowers *et al.*, 2005) in the form

$$\left.\frac{\partial^2 f_2}{\partial \hat{\beta}^2}\right|_{\beta^*} = \left.\frac{\partial^2 f_1}{\partial \hat{\beta}^2}\right|_{\beta^*} + 2\left.\frac{\partial^2 f_1}{\partial \beta \partial \hat{\beta}}\right|_{\beta^*}. \tag{B6}$$

Calculating the mixed derivative of $f_1$, by differentiating (B2) with respect to $\beta$ and evaluating at a singularity, and using $\beta S = \Gamma + c\phi P$ and (B3), gives

$$\left.\frac{\partial^2 f_1}{\partial \beta \partial \hat{\beta}}\right|_{\beta^*} = \frac{\partial I}{\partial \beta}\frac{S(cP(\phi - 1) + \alpha)(S - I)}{\beta H^3} + \frac{cI}{\beta^2 H^3}\frac{\partial P}{\partial \beta}[-\phi(cP(\phi - 1) + \alpha)(S - I) + \beta SH(\phi - 1)]. \tag{B7}$$

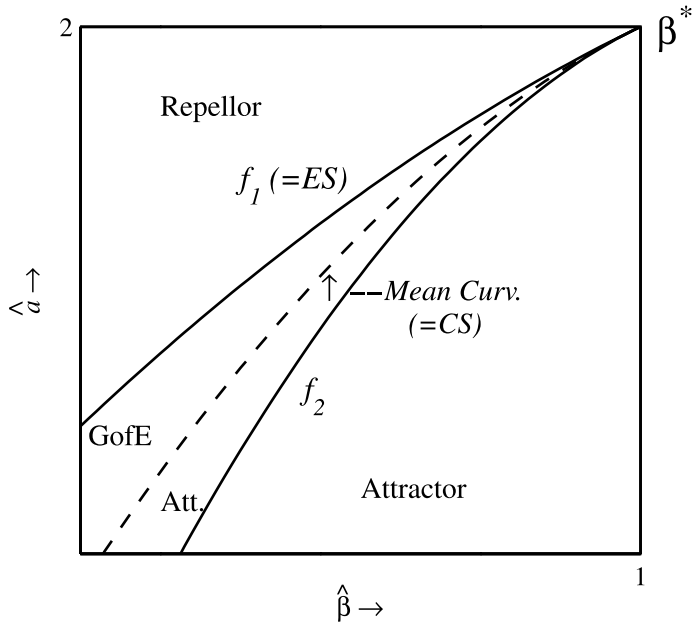


**Fig. B1.** A typical trade-off and invasion plot for a trade-off between reproduction $a$ and transmission $\beta$. Branching points are not possible for this plot as the $f_1$ invasion boundary is above the $f_2$ so that a region where the singularity is CS but not ES does not occur. [If the two invasion boundaries were swapped over, the Garden of Eden (ES-repellor) region would be replaced by a branching region.] The parameter values are $q = 0.5$, $b = 0.2$, $\alpha = 0.2$, $\gamma = 0.2$, $c = 0$, $a^* = 2$, $\beta^* = 1$.

### Predator-free environment

To explore this further, we first look at the case where the prey exists in a predator-free environment, hence $P = 0$ and $\partial P/\partial\beta = 0$. The derivative of the susceptible population is $\partial S/\partial\beta = -S/\beta$, as $S = \Gamma/\beta$. Differentiating $dH/dt$ in (1) through with respect to $\beta$, evaluating at equilibrium and solving for $\partial I/\partial\beta = 0$, using (B3) gives

$$\left.\frac{\partial I}{\partial\beta}\right|_{\beta^*} = \frac{qSH^2}{\beta(qH^2 + \alpha S)} \;\Rightarrow\; \left.\frac{\partial^2 f_1}{\partial\beta\partial\hat{\beta}}\right|_{\beta^*} = \frac{\alpha q S^2 H^2 (S - I)}{\beta^2 H^3 (qH^2 + \alpha S)}. \tag{B8}$$

We can put this, and the curvature of $f_1$ from (B4), into (B6) to get the curvature of $f_2$, and hence use (B5) to get the CS condition. Combinations of ES and CS determine the nature of the evolutionary singularity (Metz *et al.*, 1996a; Geritz *et al.*, 1998; Bowers *et al.*, 2005).

An example of how the invasion boundaries appear when plotted on a singular TIP is given in Fig. B1.

### Predator–prey–infection

To gain the results for Fig. 3, we require the CS condition for when both the predator and the infection are present, i.e. when $P > 0$ (and hence $\theta c(S + \phi I) - d = 0$) and $I > 0$ (and hence $\beta S - \Gamma - c\phi P = 0$). Returning to the original dynamical equations in (1) and differentiating

the predator and infection equations through with respect to $\beta$ we can find the derivatives of $S$ and $P$ as

$$\frac{\partial S}{\partial \beta} = -\phi \frac{\partial I}{\partial \beta} \quad \text{and} \quad \frac{\partial P}{\partial \beta} = \frac{S}{\phi c} - \frac{\beta}{c}\frac{\partial I}{\partial \beta}. \tag{B9}$$

Differentiating the dynamical equation for the total prey population gives

$$\frac{\partial}{\partial \beta}\left(\frac{dH}{dt}\right) = \frac{da}{d\beta} H + \frac{\partial H}{\partial \beta}(a - 2qH - b) - \alpha \frac{\partial I}{\partial \beta} - c\frac{\partial P}{\partial \beta}(S + \phi I) + cP\left(\frac{\partial S}{\partial \beta} + \phi \frac{\partial I}{\partial \beta}\right) = 0. \tag{B10}$$

Evaluating at an evolutionary singularity, and hence using (A3) for $da/d\beta$ (and solving for $\partial I/\partial \beta$), we get

$$\frac{\partial I}{\partial \beta} = \frac{S(-\phi I(cP(\phi - 1) + \alpha) + \beta H(S + \phi I))}{\phi \beta H[(a - 2qH - b)(1 - \phi) - \alpha + \beta(S + \phi I)]}. \tag{B11}$$

Substituting (A9) into the mixed derivative from (A8) gives

$$\left.\frac{\partial^2 f_1}{\partial \beta \partial \hat{\beta}}\right|_{\beta *} = \frac{1}{\beta H^3}\frac{\partial I}{\partial \beta}[(S + \phi I)(cP(\phi - 1) + \alpha)(S - I) - \beta SIH(\phi - 1)] + \frac{SI}{\phi \beta^2 H^3}[-\phi(cP(\phi - 1) + \alpha)(S - I) + \beta SH(\phi - 1)]. \tag{B12}$$

## APPENDIX C: NUMERICAL SIMULATIONS

Simulation analysis is used to verify the theoretical results about the position and nature of the singular point. In the simulations, the population dynamics were numerically solved for a fixed time ($t_a$) according to (1) initially with a monomorphic population. Mutant strains, those we defined by trait values $\hat{\beta}$ (and $\hat{a} = f(\hat{\beta})$), were generated by small deviations around the current trait $\beta$ (and $a = f(\beta)$) (the choice of current strain from which to mutate depends on its relative density) and introduced at low density. The population dynamics were then solved for a further time $t_a$ with strains whose total population density fell below a (very low) threshold considered extinct and removed; in addition, and a new feature for this study, if the total infection (predator) level across all strains fell below this threshold, the pathogen (predator) was considered extinct and removed, but the susceptible counterparts remained. After this removal, new mutations were created and the procedure repeated. In this way, the parameter $\beta$ (and therefore $a$ via the trade-off) could evolve. One difference between the theory and simulations is that the simulations are not mutation-limited (i.e. new mutants could evolve before previous mutants had reached equilibrium or gone extinct). Although this could be overcome by increasing $t_a$, this set-up has generally been shown to correctly approximate the evolutionary behaviour predicted by adaptive dynamics in studies where the dynamical attractor is an equilibrium point (see, for example, Hoyle *et al.*, 2011).

## APPENDIX D: DISCONTINUITY IN THE CS CONDITION

By combining (B9) and (B11), it can be shown that as $c$ goes towards the critical value that allows the predator to invade from above, and hence as $P \to 0^+$, the derivative $\partial S/\partial \beta$ does

not equal the equivalent derivative if you were to approach that same point from the other direction (see result near (B7)):

$$\left.\frac{\partial S}{\partial \beta}\right|_{P\to 0^{+}} = -\frac{\mathrm{S}}{\beta}\frac{-\phi I\alpha + \beta H(S+\phi I)}{H[(\alpha - 2qH - b)(1-\phi) - \alpha + \beta(S+\phi I)]} \neq \left.\frac{\partial S}{\partial \beta}\right|_{P\to 0^{-}} = -\frac{S}{\beta}. \qquad \text{(D1)}$$